Retinal Vessel Cannulation with an Image-Guided Handheld Robot

Brian C. Becker, Sandrine Voros, Louis A. Lobes, Jr., James T. Handa, Gregory D. Hager, and Cameron N. Riviere

***Abstract*—Cannulation of small retinal vessels is often prohibitively difficult for surgeons, since physiological tremor often exceeds the narrow diameter of the vessel (40-120 µm). Using an active handheld micromanipulator, we introduce an image-guided robotic system that reduces tremor and provides smooth, scaled motion during the procedure. The micromanipulator assists the surgeon during the approach, puncture, and injection stages of the procedure by tracking the pipette and anatomy viewed under the microscope. In experiments performed *ex vivo* by an experienced retinal surgeon on 40-60 µm vessels in porcine eyes, the success rate was 29% (2/7) without the aid of the system and 63% (5/8) with the aid of the system.**

I. Introduction

RETINAL surgery often requires manipulation of extremely small, delicate anatomy. New microsurgical procedures in the eye are yielding encouraging results in the treatment of diseases such as retinal vein occlusion (RVO). RVO occurs when a clot obstructs blood flow in a central or branch vein of the eye (CRVO and BRVO, respectively). As the second most common retinal vascular disease, RVO affects an estimated 16.4 million adults worldwide [1] and has no proven effective treatment [2].

A promising experimental surgical procedure is retinal endovascular surgery (REVS), which involves cannulating the vein and directly injecting clot-dissolving plasminogen activator (t-PA) to remove obstructions [3]. *In vivo* retinal vessel cannulations were first reported with cats and rabbits using a micromanipulator to fix the micropipette and damp hand movements [4]. Although subsequent research has demonstrated successful cannulations in a variety of animal and human models, there are difficulties involved in manipulating such tiny vessels. It has been noted that larger vessels are easier to puncture than smaller vessels more distal to the optic nerve [5]. In experiments with human cadaver eye models, Tang and Han [6] recorded that only 10 out of 18 attempted cannulations were successful and commented that manipulating vessels with currently available instrumentation is generally traumatic.

These reports are not surprising considering that physiological tremor of vitreoretinal surgeons has been measured at over 100 µm in amplitude [7], which is greater than the typical 40-120 µm diameter of retinal vessels. Recognizing the need for reduced tremor and increased precision, [8] describes cooperative control between a surgeon and a Steady-Hand robot for *in vivo* cannulation of 80 µm vessels in the chorioallantoic membrane of chicken embryos. Though the approach did not improve the cannulation success rate, the experiment did show improved ability to maintain the cannula in the vessel. We propose a vessel cannulation system based on a handheld robot, "Micron" [9], using vision-based control. Preliminary results *ex vivo*, performed by an experienced retinal surgeon, validate the system.

II. Methods

The vessel cannulation system integrates a micromanipulator with stereo cameras mounted on a high-magnification microscope. By tracking the micropipette tip and vessels, tremor compensation can be combined with motion scaling to give the surgeon increased precision in the vicinity of the targeted vessel during the procedure.

A. Micron

Micron, depicted in Fig. 1, is a 3-DOF actuation micromanipulator with 6-DOF sensing for locating the instrument's tip and orientation [9]. Being a fully handheld device with Thunder® piezoelectric actuators (Face International Corp., Norfolk, VA., USA) located between the handle grip and end-effector, Micron can position the tip within an approximate 3.0 x 3.0 x 0.8 mm range centered on the null position. The null position of the micromanipulator is defined as the unactuated position of the tip, or where the

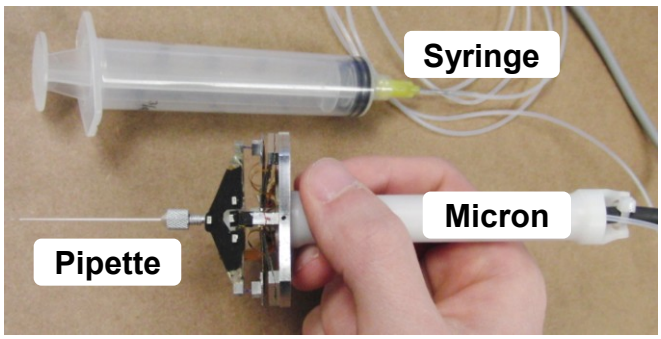

Fig. 1. Micron handheld micromanipulator with glass pipette attached with tubing to a 20 mL syringe.

This work was supported in part by the National Institutes of Health (grant nos. R01 EB000526, R21 EY016359, and R01 EB007969), the American Society for Laser Medicine and Surgery, the National Science Foundation (Graduate Research Fellowship), and the ARCS Foundation.

B. C. Becker and C. N. Riviere are with the Robotics Institute, Carnegie Mellon University, Pittsburgh, PA 15213 USA (e-mail: camr@ri.cmu.edu).

S. Voros and G. D. Hager are with the Computer Science Department, Johns Hopkins University, Baltimore, Maryland 21218 USA.

L. A. Lobes, Jr., is with the Department of Ophthalmology, University of Pittsburgh Medical Center, Pittsburgh, PA 15213 USA.

J. T. Handa is with the Wilmer Eye Institute, Johns Hopkins University, Baltimore, Maryland 21218 USA.

tip would be if the power were off. Custom optical tracking hardware uses Position-Sensitive Detectors (PSDs) to track three pulsed LEDs attached to the shaft of the instrument and one pulsed LED attached to the handle. By measuring the locations of the LEDs, pose information of both the tool tip and handle are reconstructed at 2 kHz with a precision of approximately 10 μm RMSE.

B. System Setup

As shown in Figs. 1 and 2, the surgeon uses Micron in a 2x3 mm workspace under a Zeiss OPMI® 1 microscope at 25X magnification. An optical bridge splits the microscope view between the microscope eyepieces and two Flea®2 cameras (Point Grey Research, Richmond, BC, Canada). Mounted as a stereo pair, the cameras capture 800x600 resolution video at 30 Hz. For cannulation procedures, TIP1TW1 micropipettes (World Precision Instruments, Saratoga, FL, US) with an inner diameter (ID) of 1 μm are secured to the output plate of Micron. Tubing threads through the hollow center of Micron's shaft and connects to a 20 mL syringe, which can be depressed to force gas or fluid through the micropipette and into the vessel.

C. Vision System

The stereo cameras are responsible for tracking both the tip of the micropipette and the vessels in the image to ascertain the proximity of the micropipette to the vessel as depicted in Fig. 3. The relative distance is used by the control system, which adjusts the scale factor that determines how much hand motion is transferred from the handle to the tip of the instrument.

Since the micropipettes are formed from clear glass and the tip tapers off to a nearly invisible point, directly tracking the tip with vision poses a significant challenge. As an effective alternative, two unique colored fiducials are painted in stripes around the micropipette near the tip. Fast color segmentation [10] tracks the centroids of the fiducials,

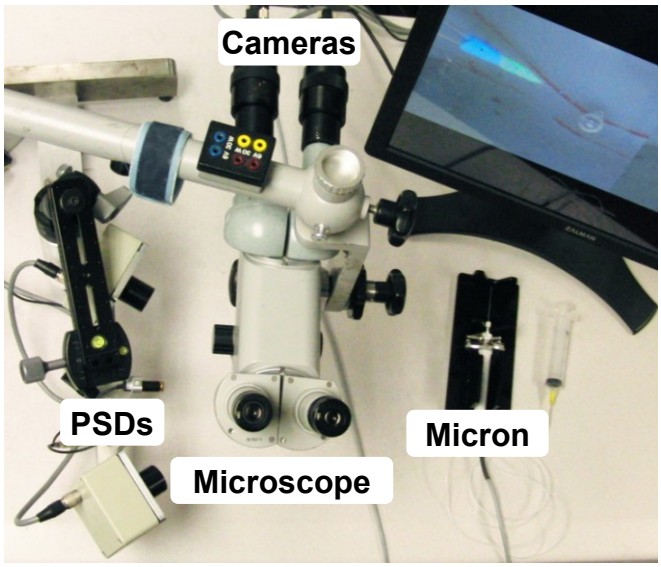

Fig. 2. Cannulation setup with Micron micromanipulator, microscope, stereo cameras, and PSD optical sensors.

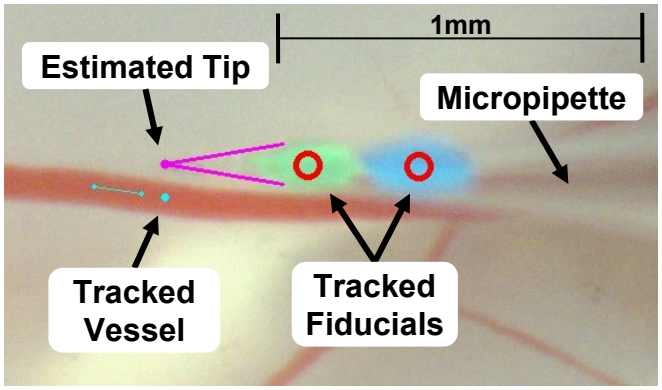

Fig. 3. Stereo cameras track 3D positions of green and blue fiducials on the micropipette to estimate the tip position. The vision system also detects vessels in the image to calculate the center of the vessel nearest the micropipette tip. *Figure best viewed in color.*

and the true micropipette tip position is estimated with interpolation. A quick 30 s calibration period registers the camera views with the world coordinate system as defined by the PSDs measuring the 6-DOF pose of the instrument; registration is maintained by an online adaptive least squares calibration procedure that adjusts the camera coordinate system to the world frame with each new camera image.

Vessels are similarly tracked with a Gaussian Mixture Model of learned vessel colors [11]. By searching locally around the estimated position of the micropipette tip, the XY center of the nearest vessel is located. Because vessels appear as locally invariant structures, i.e., one section of the vessel does not look significantly different from another section, correspondences for 3D reconstruction of the vessel are difficult to find. Instead, a global estimate of the mean depth Z of all blood vessels in view is calculated by running a simplified Lucas-Kanade tracker [12], which estimates the translation between the left and right camera views of the blood vessels. The 3D distance between the micropipette tip and the center of the nearest vessel as calculated by the stereo cameras is then given to the control system.

D. Tremor Compensation and Motion Scaling

Two key components form basis of the control system: tremor compensation and motion scaling. Hand tremor is compensated by commanding the micromanipulator tip $P_T \in \mathbb{R}^3$ to the the null position $P_N \in \mathbb{R}^3$ that has first been filtered by a lowpass filter $\boldsymbol{F_L}$. Since the null position is mechanically tied to the handle, the micropipette tip output is the smoothed input of the operator's hand movements:

$$P_T = \boldsymbol{F_L}(P_N) \qquad (1)$$

Since physiological hand tremor generally lies in a frequency band of 8-12 Hz, a first-order 1.5 Hz lowpass Butterworth filter was selected for $\boldsymbol{F_L}$, which greatly attenuates tremor while only introducing a minor lag and settling time into the eye-hand coordination feedback loop.

The second key component used by the control system is motion scaling, which gives the surgeon increased precision. Motion scaling takes the handle motion as calculated by the change in null position ΔP_N and transfers only a fraction

$1/s \in \mathbb{R}$ of the movement to the micromanipulator tip ΔP_T:

$$\Delta P_T = \frac{1}{s}\Delta P_N \qquad (2)$$

For example, if the scale factor is 2 and the surgeon moves the handle 100 μm, the tip only moves 50 μm. Any uncompensated tremor, drift, or deliberate movement is scaled down, granting the surgeon the additional comfort and safety of using larger movements to manipulate tiny anatomy. A scale factor of unity is equivalent to running no motion scaling (i.e., Micron turned off) while a scale factor of ∞ corresponds to fixing the tip in space (i.e., disregarding all operator's movement).

One important limitation of motion scaling is the decreased range of motion. During tremor compensation, the lowpass filter gain rolls off to unity at 0 Hz so the manipulator range of motion is only used temporarily to smooth out sudden jerks and/or tremor. However, since motion scaling is applied all the way down to 0 Hz, the effective range of motion of the device is reduced by a factor s. For this reason, tremor compensation can be performed everywhere, whereas motion scaling can only be applied in a limited volume, generally near the vessel where it is most effective in aiding the cannulation procedure.

Additionally, because the 0.8 mm axial range of Micron is significantly smaller than the 3.0 mm transverse range, motion scaling is applied anisotropically. While tremor compensation is applied in all directions at all times, motion scaling is only activated as discussed earlier in the vicinity of the vessel and only in the transverse directions of the tool. In addition to preserving manipulator range along the axis of the tool where the range of motion is most limited, anisotropic scaling has an additional benefit. Since the surgeon approaches the vessel along a roughly parallel trajectory, unity motion scaling axially allows for quick thrusts into the vessel while motion scaling in the transverse direction increases the ability of the surgeon to keep the micropipette centered on the vessel.

E. Control System

The control system combines tremor compensation with anisotropic motion scaling to aid the surgeon in cannulation procedures. Tremor compensation is applied at all times for smooth movements. Motion scaling is activated only when the micropipette is closer than a certain threshold to the vessel, as measured by the vision system. A threshold value of 500 μm was selected empirically. Although motion scaling could be implemented with a velocity controller, estimation of the velocities from measured positions is noisy. A preferable approach in our system is to select some reference point $P_R \in \mathbb{R}^3$ for motion scaling, measure the offset between the tremor-compensated null position $\boldsymbol{F_L}(P_N)$ and the reference point P_R, and use a position controller to drive the micromanipulator tip P_T to the measured offset position, scaled by $1/s$. Anisotropic motion scaling is achieved by taking into account the rotation $R \in \mathbb{R}^{3\times3}$ of the tool, and introducing individual scale factors s_X, s_Y, and s_Z:

$$S = \begin{bmatrix} 1/s_X & 0 & 0 \\ 0 & 1/s_Y & 0 \\ 0 & 0 & 1/s_Z \end{bmatrix}; s_X, s_Y, s_Z \in [1, \infty] \qquad (3)$$

$$P_T = S(R\boldsymbol{F_L}(P_N) - RP_R) + RP_R$$

The reference point P_R is selected as the tremor compensated null position at the time of activating motion scaling $P_R = \boldsymbol{F_L}(P_N)$ and held constant until scaling is deactivated.

As the operator moves Micron during the procedure, the motion scaling displaces the tip away from the null position, reducing the range of motion. At some point, the micromanipulator tip must return to the null position, otherwise the actuators will saturate and Micron will be unable to provide any assistance. Ideally, we would prefer sufficient range of motion to complete the cannulation and withdraw from the vessel before returning the tip to the null position, thus maximizing the range for other operations.

Turning off motion scaling is done when the vision system senses the tip has left the vicinity of the vessel (i.e., the distance between them exceeds a certain threshold). However, directly commanding the micromanipulator tip to the null position causes a rapid and unpleasant twitch in the tool tip. Furthermore, transient tracking errors may falsely trigger turning off the motion scaling. Since tracking is not entirely reliable, the problem of determining when and how to return to pure tremor compensation is exacerbated.

The proposed solution involves a graceful transition from motion scaling to tremor compensation while at the same time gradually re-centering the manipulator at the null position. To account for noisy tracking, the scale is decreased exponentially over time, providing robustness to intermittently noisy or incorrect distance measurements. Denoting t as the number of successive time steps the vision system has detected the tip outside the vicinity of the vessel, the scale factor for each direction is reduced at each time step:

$$s_D \leftarrow s_D - \frac{\alpha}{(1+\gamma)^t} \; \forall D = \{X, Y, Z\} \qquad (4)$$

where α specifies how much to reduce the scale at each time-step. An exponential discount factor γ encodes a sense of how confidence over time increases the convergence rate. Thus, several intermittent noisy measurements will only decrease motion scaling slightly. In contrast, a sequence of measurements indicating that motion scaling is no longer needed signifies a much higher confidence and effects a higher convergence rate back to tremor compensation. Equation (4) terminates for each direction when the scale factor is unity, at which point the manipulator tip has returned to the null position. Alternatively, (4) terminates if the tip is re-detected within the vicinity of the vessel, in which case the reference point P_R is recalculated as:

$$P_R = (S - I)^{-1}\left(SRP_T - R\boldsymbol{F_L}(P_N)\right) \qquad (5)$$

and the scale factor is reset to avoid discontinuous jumps in

TABLE I
CANNULATION RESULTS FOR 40-60 MICRON DIAMETER VESSELS

Trials	Total Experiments	Successful Experiments	Successful Duration (s)
Unaided	7	2 (*29%*)	76 ± 31
Aided	8	5 (*63%*)	72 ± 19

Results of cannulation experiments for 40-60 µm vessels, showing the total number of cannulations attempted, the number of successful trials, and the mean ± standard deviation of the duration of successful trials.

tip position due to changing scale factors. Thus, the control system accomplishes a gentle transition from motion scaling to tremor compensation in a way that robustly deals with noise. Empirical testing indicates values of $\alpha = 3 * 10^{-5}$ and $\gamma = 1 * 10^{-4}$ are effective for a smooth 4–8 s transition.

III. EXPERIMENTS & RESULTS

Cannulation experiments were performed ex vivo by an experienced retinal surgeon under two scenarios: Aided (with the assistance of Micron) and Unaided (freehand, with Micron powered off).

A. Experimental Protocol

Porcine eyes were used as the animal model for all experiments. Sections of the back eye around the optic nerve were removed with the retina and vessels still attached. Vessel diameters were measured before each cannulation attempt, and total cannulation duration was recorded. Total duration excludes time spent clearing any bubbles in the vitreous caused by failed injections. Injections were performed by depressing a 20 mL syringe of air connected to the micropipette. The surgeon performed the insertion of the cannula into the vessel and orally indicated when to depress the syringe. Multiple injection attempts were allowed per trial. Successful cannulation was defined as air entering the vessel and displacing the blood; a cannulation was recorded as a failure when the vessel became too damaged to continue. Trials alternated between several Unaided attempts and several Aided attempts to limit ordering effects.

B. Results

As seen in Table I, for vessels with diameters between 40 and 60 µm, the cannulation success rate was higher with similar durations in successful trials. Vessels larger than 60 µm exhibit more equal success rates. Visually, Fig. 4 presents the paths inscribed by the micropipette tip during cannulation as traces on the image for both the Aided and Unaided cases. From these images, it can be seen that tremor is lessened and the surgeon's can better track the vessel in the Aided case, thus reducing trauma to the vessel and surrounding tissue.

IV. DISCUSSION

In these preliminary surgeon experiments, the robot aid of tremor compensation with motion scaling applied by the active handheld micromanipulator increased the success rate of small vessels while maintaining similar procedure duration. Better tracking algorithms could further increase

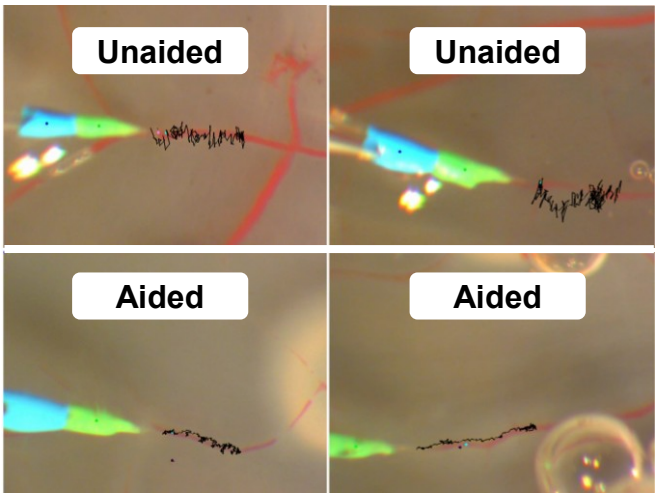

Fig. 4. Example traces of the micropipette tip during cannulation overlaid onto microscope images, showing tremor during the procedure without Micron (Unaided) and with Micron (Aided).

effectiveness. Future work will verify statistical significance with increased sample size during testing *in vivo* in chick embryo chorioallantoic membrane [13] and examine the effect of task learning curves as the surgeon becomes more proficient with both Aided and Unaided test scenarios.

REFERENCES

[1] R. Sophie, L. M. Rachel, C. Ning, L. Lyndell, W. Jie Jin, M. Paul, W. K. Jonathan, N. Hiep, and Y. W. Tien, "The prevalence of retinal vein occlusion: Pooled data from population studies from the United States, Europe, Asia, and Australia," *Ophthalmology,* vol. 117, pp. 313-319.e1, 2010.

[2] B. Nilufer and B. Cosar, "Surgical treatment of central retinal vein occlusion," *Acta Ophthalmologica,* vol. 86, pp. 245-252, 2008.

[3] L. A. Bynoe, R. K. Hutchins, H. S. Lazarus, and M. A. Friedberg, "Retinal endovascular surgery for central retinal vein occlusion: Initial experience of four surgeons," *Retina,* vol. 25, pp. 625-32, 2005.

[4] B. Allf and E. de Juan, Jr., "In vivo cannulation of retinal vessels," *Graefes Arch. Clin. Exp. Ophthalmol.,* vol. 225, pp. 221-225, 1987.

[5] M. K. Tsilimbaris, E. S. Lit, and D. J. D'Amico, "Retinal microvascular surgery: A feasibility study," *Invest. Ophthalmol. Vis. Sci.,* vol. 45, pp. 1963-1968, June 2004.

[6] W. M. Tang and D. P. Han, "A study of surgical approaches to retinal vascular occlusions," *Arch. Ophthalmol.,* vol. 118, pp. 138-143, 2000.

[7] S. P. N. Singh and C. N. Riviere, "Physiological tremor amplitude during retinal microsurgery," in *Proc IEEE 28th Annu. Northeast Bioeng. Conf.*, 2002, pp. 171-172.

[8] I. Fleming, M. Balicki, J. Koo, I. Iordachita, B. Mitchell, J. Handa, G. Hager, and R. Taylor, "Cooperative robot assistant for retinal microsurgery," *Lect. Notes Comput. Sci.,* vol. 5242, pp. 543-550, 2008.

[9] J. C. Tabarés, R. A. MacLachlan, C. A. Ettensohn, C. N. Riviere, "Cell Micromanipulation with an Active Handheld Micromanipulator," *Proc IEEE EMBC*, 2010, accepted for publication.

[10] J. Bruce, T. Balch, and M. Veloso, "Fast and inexpensive color image segmentation for interactive robots," in *Proc. IEEE/RSJ Int. Conf. Intell. Rob. Syst.*, 2000, pp. 2061-2066.

[11] M.-H. Yang and N. Ahuja, "Gaussian mixture model for human skin color and its applications in image and video databases," *Proc. SPIE,* vol. 3656, pp. 458-466, 1998.

[12] S. Baker and I. Matthews, "Lucas-Kanade 20 years on: A unifying framework," *Int. J. Comput. Vis.,* vol. 56, pp. 221-255, 2004.

[13] T. Leng, J. M. Miller, K. V. Bilbao, D. V. Palanker, P. Huie, and M. S. Blumenkranz, "The chick chorioallantoic membrane as a model tissue for surgical retinal research and simulation," *Retina,* vol. 24, pp. 427-434, 2004.